Optica Applicata, Vol. XXXV, No. 2, 2005

Hyperpolarized ^{3}He gas production by metastability exchange optical pumping for magnetic resonance imaging

KATARZYNA SUCHANEK[1], KATARZYNA CIEŚLAR[1], ZBIGNIEW OLEJNICZAK[2], TADEUSZ PAŁASZ[1], MATEUSZ SUCHANEK[1], TOMASZ DOHNALIK[1]

[1]Institute of Physics, Jagiellonian University, Reymonta 4, 30-059 Kraków, Poland

[2]Institute of Nuclear Physics, Polish Academy of Sciences, Radzikowskiego 152, 31-342 Kraków, Poland

A portable ^{3}He gas polarizer based on metastability exchange optical pumping is described. It produces 75 ml of highly polarized ^{3}He gas at the pressure of 100 mbar, by implementing a non-magnetic peristaltic compressor, which transfers the ^{3}He gas from the low-pressure optical pumping cell to the storage cell. About 30% polarization at 1 mbar is achieved in the optical pumping cell in a single run, and 20 compression cycles are needed to reach the final pressure in the storage cell. After adding a buffer gas up to the atmospheric pressure, the mixture is used in magnetic resonance imaging (MRI) experiments. Preliminary images of phantoms and of the rat lungs *in vivo* confirm the usefulness of the ^{3}He gas polarizer in MRI applications.

Keywords: hyperpolarized ^{3}He, lung imaging, low field MRI.

1. Introduction

Hyperpolarized ^{3}He has recently become an important contrast agent for magnetic resonance imaging (MRI) of empty cavities in the body (lungs, sinuses) [1, 2] and in porous media [3]. Since conventional proton MRI of air spaces suffers from low proton density and large susceptibility differences at the air-tissue interface, the ^{3}He-MRI has gained significant interest as a new diagnostic tool for functional and morphological studies of lungs. First images of guinea pig lungs using this technique were obtained in 1995 [4]. Soon thereafter, the images of the human lungs filled with hyperpolarized ^{3}He were obtained [5, 6]. Since then the method has been improved and applied both to animal models of embolism and emphysema [7, 8], and to clinical studies on volunteers and patients [1].

One of the main advantages of ^{3}He-MRI is high polarization level of ^{3}He nuclear spins, which is five orders of magnitude greater than the thermal polarization at a typical magnetic field used in MRI. The hyperpolarization is achieved by means of optical pumping [9] – a technique of transferring angular momentum from photons to

atoms by resonant absorption of circularly polarized light. The high polarization level (of the order of 1) overcomes lower density of gas in the lungs as compared to proton density in tissues. Hence good quality images can be obtained even at low magnetic field [10–12]. However, the non-equilibrium polarization of the hyperpolarized gas achieved in this way requires some specific storage and handling issues to be solved. For medical applications, a fast accumulation of large amount of helium gas with high degree of nuclear polarization is desirable. In this work we describe a home-built optical polarizer, storage, and handling unit, to be used in low field MRI of small animal lungs.

The paper is organized as follows. In Section 2 relevant points of metastability exchange optical pumping of ^{3}He are given. Section 3 is concerned with the home -built portable gas production system, which can be used in a hospital environment. A dedicated, low field MRI system for small animal lungs imaging, which is based on the permanent magnet, is briefly described in Sec. 4. Recent experimental results of imaging several phantoms filled with hyperpolarized gas, as well as the first *in vivo* images of the rat lungs are shown in Sec. 5. The paper is concluded with the discussion of possible future applications of hyperpolarized ^{3}He-MRI.

2. Hyperpolarization of ^{3}He

To produce hyperpolarized ^{3}He gas for MRI, two optical pumping methods are currently employed, namely spin exchange optical pumping (SEOP) [13], and metastability exchange optical pumping (MEOP) [14]. In the SEOP, nuclear polarization of ^{3}He atoms is achieved during their collisions with optically pumped alkali-metal atoms (*e.g.*, rubidium). The process occurs at high temperature (80–160°C), under a pressure of the order of 1 bar. In the MEOP, the ^{3}He atoms in the ground state are polarized by collisions with optically pumped ^{3}He atoms in the metastable state. The MEOP involves helium atoms only at room temperature and at low pressure, of the order of few mbars.

Both techniques are used nowadays. The main advantage of MEOP method is that it results in a pure ^{3}He gas and requires no intermediate medium to transfer the angular momentum from photon to ^{3}He atom. The chemical purity of hyperpolarized ^{3}He gas is critical in medical applications. The process of MEOP is very efficient (high polarization rate), thus the characteristic polarization time for MEOP is of the order of seconds, instead of several hours necessary in SEOP at comparable laser power. However, MEOP is accomplished at a relatively low pressure, so the polarization -preserving compression of the gas up to atmospheric pressure is needed. Adding a buffer gas (*e.g.*, ^{4}He, N_2) is another possibility, but in this case a significant dilution of hyperpolarized gas is disadvantageous as far as the sensitivity of MRI is concerned. On the contrary, SEOP requires no further compression, since the optical pumping occurs at high gas pressure.

As a matter of fact, the choice of polarization method depends also on the actual equipment one has at his disposal to perform optical pumping, especially the

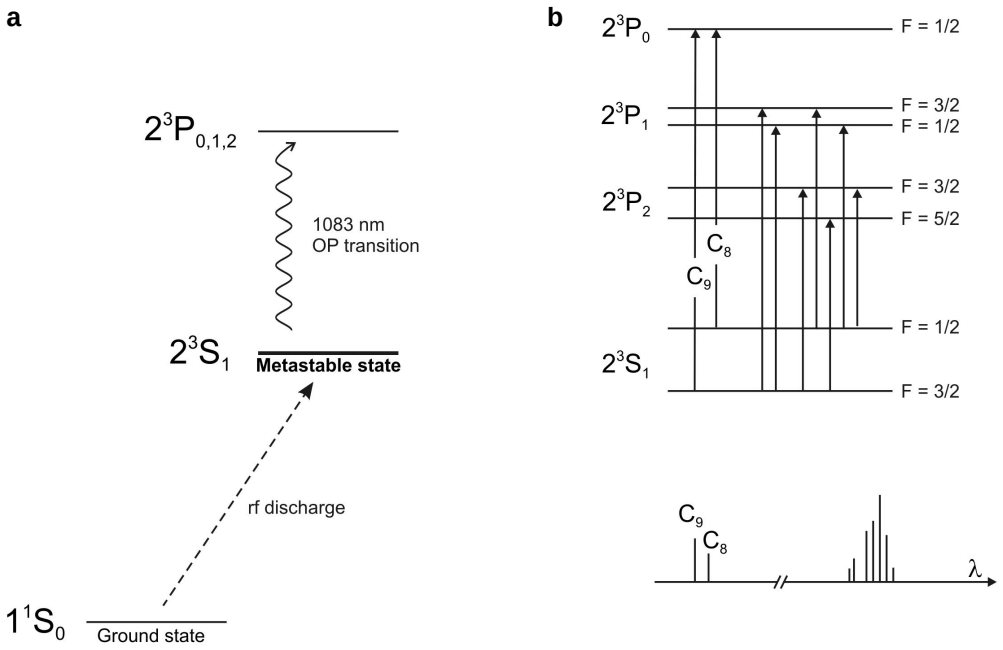

Fig. 1. Low-lying energy levels of ^{3}He (**a**). Components of the hyperfine structure of ^{3}He emission line λ = 1083 nm (**b**).

wavelength and power of available laser. In our laboratory we produce hyperpolarized ^{3}He by means of MEOP, because a non-expensive 50 mW DBR diode laser of the wavelength of 1083 nm is available. In the following we present the principle of this method and technical details of its implementation.

The MEOP process takes place in a homogeneous guiding magnetic field, which is needed to establish the quantization axis only. The low-lying energy levels of ^{3}He are presented in Fig. 1**a**. Since ^{3}He nuclei have spin $I = 1/2$, the atomic states have hyperfine structure with sublevels characterized by various m_F quantum numbers. The optical transitions between 2^3S_1 and 2^3P states correspond to resonant line of ^{3}He with the wavelength λ = 1083 nm. The components of the hyperfine structure of this line are depicted in Fig. 1**b**. The process of MEOP starts with populating the 2^3S_1 metastable state. This is achieved through a weak rf discharge, because the optical transition between 2^3S_0 and 2^3S_1 states is strictly forbidden. The lines C_8 and C_9 are most commonly employed for optical pumping. We explain the process of using the C_8 transition in more detail.

The absorption of right-hand circularly polarized (σ^+) laser beam causes transitions from 2^3S_1 ($m_F = -1/2$) to 2^3P_0 ($m_F = +1/2$) state (Fig. 2). After excitation, a spontaneous reemission to both sublevels of 2^3S_1 state occurs. However, the continuous depletion of the $m_F = -1/2$ sublevel results in higher population of the 2^3S_1, $m_F = +1/2$ state. This is equivalent to the net polarization of the total angular momentum of the metastable atoms.

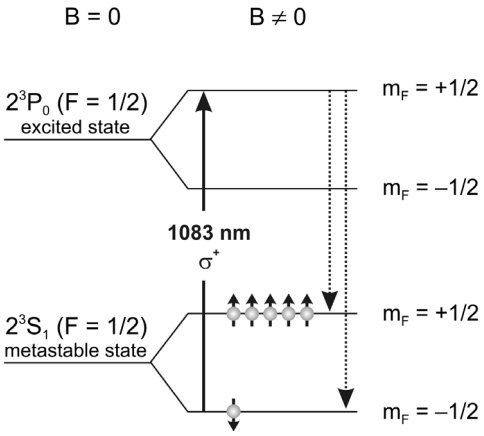

Fig. 2. Schematic diagram of the optical pumping using C_8 component of 2^3S_1–2^3P helium transition. Right-hand circularly polarized light (σ^+) can only excite the transition with angular momentum selection rules $\Delta m_F = +1$. As a result the $m_F = -1/2$ state is depopulated and all population is transferred to the $m_F = +1/2$ state.

Nuclear polarization of the ground state ^{3}He atoms is achieved via so-called metastability exchange collisions. During that process a polarized metastable atom and a non-polarized ground state atom exchange their electronic states, while the nuclear polarization stays unaffected. As a result one obtains an atom in a ground state with the polarized nucleus, and a new metastable atom that can be further optically pumped by the laser. A continuous application of the rf discharge and the laser radiation leads to the equilibrium polarization, the magnitude of which depends on several parameters such as metastable atom density, polarization build-up time, and the relaxation rate of polarized atoms. The latter depends on laser power, pumping transition, gas pressure and intensity of discharge.

3. Gas production system

The gas production system is presented in Fig. 3. The magnetic field is generated by a set of six coaxial coils, which produces a homogeneous field of the order of 25 G in a sufficiently large volume to accommodate a cell where the optical pumping takes place (OP cell), as well as a storage cell (S cell). The estimated homogeneity of the magnetic field within the working volume is about 150 ppm. The OP cell has a form of 15 cm long cylinder, of 5 cm diameter. The storage cell can accumulate up to 75 ml of gas at the atmospheric pressure. Both cells are made of glass with reduced iron concentration, to minimize interactions of spin-polarized ^{3}He atoms with the paramagnetic centers on the inner surface of the containers walls, which leads to so-called wall relaxation [15].

To perform optical pumping, the OP cell has to contain pure ^{3}He in order to produce large amount of atoms in 2^3S metastable state that can absorb resonant laser beam.

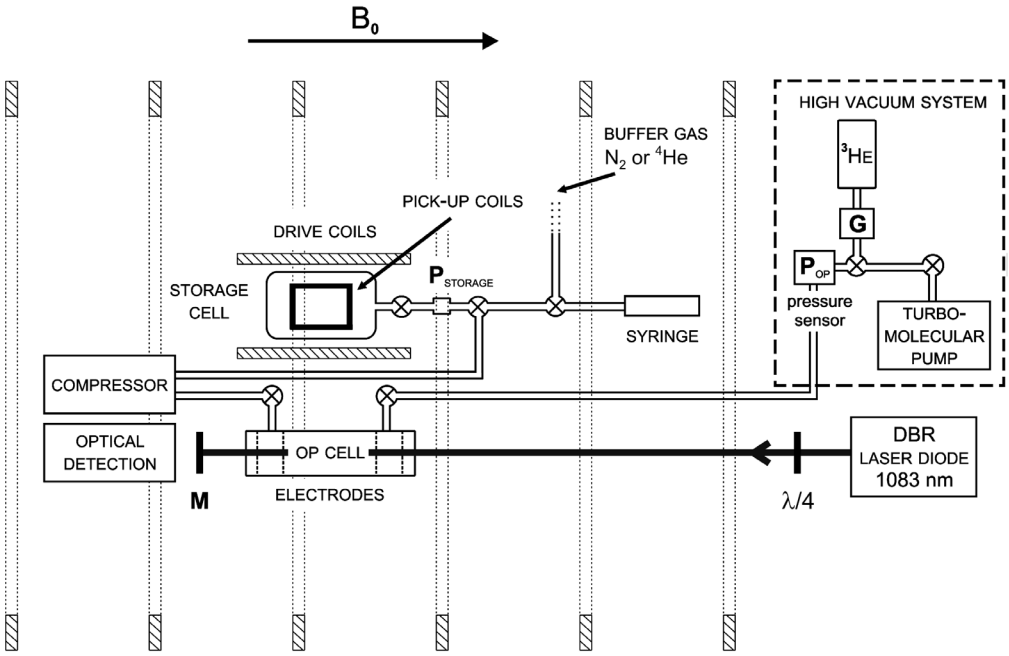

Fig. 3. Schematic view of the high-efficiency optical polarizer. The low pressure part includes turbomolecular pump, bottle of ^{3}He, getter G, pressure sensor to control the pressure inside OP cell P_{OP} and OP cell. Optical pumping is performed using DBR laser diode. The laser beam is circularly polarized using quarter wave plate ($\lambda/4$) and is back reflected by the dielectric mirror M. The gas is pumped by the compressor from the OP cell to the high pressure section and is accumulated in the storage cell.

Any impurity of the gas can contribute to electronic relaxation of the metastable state. For this reason the OP cell first undergoes a standard cleaning procedure, which comprises an overnight heating and a following application of strong discharge to remove all undesirable atoms and molecules from the cell walls. After completing the preliminary cleaning, the cell is connected to a high vacuum system using glass tubes of about 6 mm internal diameter, which allow to obtain high flux. The bottle of high purity ^{3}He gas (99.999%) is used for all experiments. Further cleaning of ^{3}He gas is achieved by using a getter and mechanical filter on the way from the gas bottle to the OP cell. The high vacuum system includes the turbo molecular pump that can achieve the vacuum of the order of 10^{-7} mbar. The pressure inside the OP cell is controlled by a capacitance pressure sensor (Keller, Holand) and allows to fill the OP cell with the precisely defined amount of gas. All connections within the high vacuum system are made of stainless steel. The commercial joints between the steel and glass parts are applied (Swagelok, USA).

A high population of helium atoms in the 2^3S metastable state is created by a weak rf discharge, which is produced by four electrodes wrapped around the cell. The electrodes are driven by a 3 MHz, 10 W rf power amplifier through a matching transformer. A DBR laser diode (SDL-6702-H1) delivering up to 50 mW of output

power is used for optical pumping. The laser beam passes through the cell once and then is reflected back by a dielectric mirror to increase the efficiency of optical pumping process. The nuclear polarization inside the OP cell is measured by an optical polarimeter, which is mounted on the laser axis, as shown in Fig. 3. The optical method for determining of the nuclear polarization is based on the analysis of the degree of circular polarization of the red (668 nm) light emitted by the discharge in the cell [16]. During the discharge sustained in the gas, the helium atoms can be transferred to various excited levels without perturbing nuclear spin. The hyperfine interaction mixes the nuclear and the electronic polarization. The result of mixing manifests itself in the spontaneous emission as a degree of circular polarization, which is related directly to the nuclear polarization.

The dielectric mirror used has the reflection coefficient of about 99.9% for 1083 nm wavelength, but transmits the visible part of the spectrum. Thus it is possible to collect the light from the excited helium plasma onto the photodiode inside the polarimeter. In order to improve the sensitivity, the lock-in technique is used by applying a low frequency modulation to the rf discharge, and simultaneously using the modulation signal as the reference. This technique of measuring the nuclear polarization of ^{3}He is limited to low magnetic field and low gas pressure, and requires the maintenance of the discharge during measurements.

After the optical pumping process in the OP cell has been completed, the gas is transferred to the S cell using a non-magnetic peristaltic compressor [17]. It is driven by a standard electric motor mounted 75 cm away from the polarizing system in order to avoid the magnetic field gradients which may cause some depolarization of the gas. In standard conditions the compressor is driven at 7 cycles/s resulting in the gas flow of about 5 cm^3/s. The pressure inside the S cell is monitored by additional pressure gauge (mounted close to the entrance to the S cell). The purity of the gas in the S cell is not so important as in the OP cell. Therefore all connections from the compressor to the S cell are made of silicon tubes and the cell is evacuated by the preliminary rotary pump only. Short tubes with small internal diameter of about 1.2 mm are used to minimize the volume and to increase the transport rate at the same time.

To monitor the nuclear polarization inside the S cell, a dedicated, low frequency pulse NMR spectrometer was built (Larmor frequency equal to 90 kHz). It is schematically shown in Fig. 3. The transmitting coil of Helmholtz type is orthogonal to B_0 and produces a homogeneous B_1 rf field within the volume of the cell. The receiving coil consists of two square sections located very close to the cell, orthogonally both to B_0 and B_1, to reduce an rf coupling between the transmitter and receiver coils. Additionally, a third section of identical geometry but of doubled number of turns is connected in series with the receiving coil in such a way that the external electromagnetic field generates the electromotive force in opposite direction. This cancels out any external electromagnetic interference, which can be rather strong at such low resonance frequency. A small tilting angle rf pulse applied to the transmitting coil causes precession of nuclear magnetization. This in turn induces a free induction decay (FID) signal in the receiving coil, which can be fed directly to

the digital lock-in, owing to relatively low precession frequency. A proper gating circuitry protects the detection system during the rf pulse and turns off the rf discharge during the NMR data acquisition.

4. MRI system

All imaging experiments were performed on a low field MRI system that has been specially designed for imaging small animal lungs using hyperpolarized ^{3}He described in detail in [18]. It is based on a permanent magnet (AMAG, Poland) of unique geometry, which gives access to the working volume from all directions and produces a magnetic field of 88 mT. It makes use of a new generation Nd-B-Fe magnetic material, which provides very high magnetic energy density. Due to the low Curie temperature of the magnetic material used, the temperature dependence of the magnetic field is about –836 ppm/°C, which made it necessary to stabilize the temperature of the magnet to ±0.1°C inside the Faraday cage. The Faraday cage simultaneously provides sufficient electromagnetic shielding at the resonance frequency of 2.84 MHz for ^{3}He and 3.73 MHz for ^{1}H. The final temperature compensation is achieved by measuring the temperature of the magnet pole and applying a correcting current to the auxiliary coil. The residual, long term temperature variations were reduced to below 15 ppm. For imaging purposes the inhomogeneity of the main magnetic field of the order of 10 ppm is required. In our system the initial inhomogeneity in a 10 cm

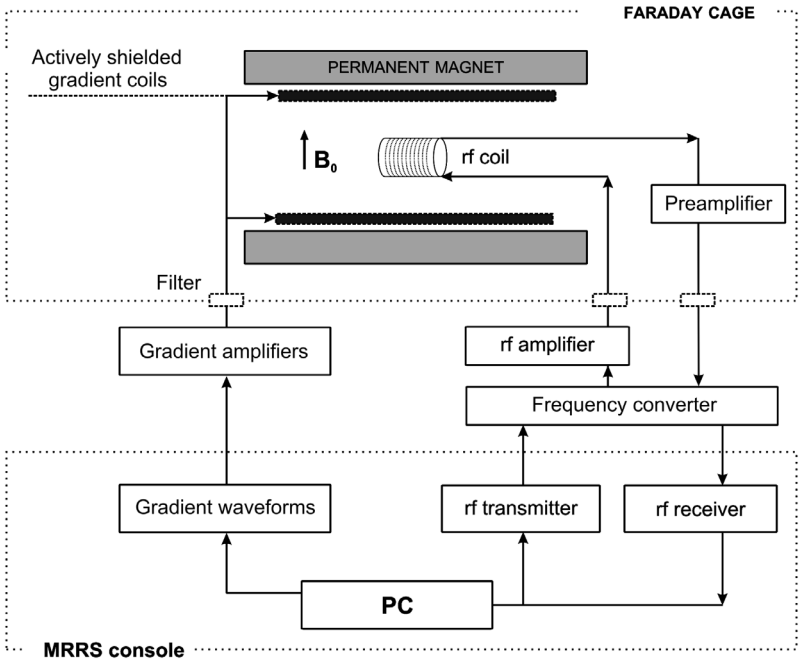

Fig. 4. Schematic view of the 88 mT MRI system.

diameter sphere (working volume) was 360 ppm. It was reduced to about 50 ppm by passive shimming, using about 50 steel pieces attached to the magnet poles as described elsewhere [18].

The magnet is equipped with a set of biplanar, actively shielded gradient coils designed and built in the Institute for Biodiagnostics (NRC, Winnipeg, Canada). The gradient strengths are about 30 mT/m at maximum current of 40 A, for all three directions. The minimum rise time for the gradient pulses is 200 μs. The gradient coils are cooled by temperature stabilized water circulating in the closed loop, and by the forced air circulation between the gradient coils assembly and the magnet poles.

The NMR signal detection is accomplished using a dual-frequency solenoid coil. It is supplemented by an additional pair of paraxial coils, producing the B_1 field within the working volume of better than 1% homogeneity. The coil can be quickly switched between the ^{3}He and ^{1}H resonance frequency, so that the complementary images can be obtained on the same object.

All MRI experiments were controlled using a commercial MR Research Systems (previously SMIS, Surrey, Great Britain) MR4200 Narrow Band console. To enable experiments on both ^{3}He and ^{1}H frequencies, the console was supplemented by a home-built frequency converter. The standard library of imaging sequences has been enhanced by special imaging protocols that are suitable for imaging small animal lungs using hyperpolarized ^{3}He. The schematic view of the MRI system is shown in Fig. 4. More technical details are given elsewhere [18].

5. Results and discussion

Since the nuclear polarization of ^{3}He obtained by optical means is non-renewable, the rf flip angle α has to be determined in the first place. It has to be kept small in all testing procedures to preserve enough polarization for further experiments. For this purpose a sealed cell filled with 2 mbar of pure ^{3}He was used. One can then perform optical pumping repeatedly, without loosing gas for accumulation. The procedure starts with applying the rf pulse (pulse duration 4.6 ms, amplitude 0.78 V), and the resulting FID signal is recorded. This operation is repeated several times until sufficient number of data points is obtained. The FID signal amplitude S_n is then proportional to:

$$S_n \sim M_0 \cos^n(\alpha) \sin(\alpha).$$

We see that $\ln S_n$ plotted as a function of n gives the straight line with a slope which yields the flip angle α to be 22.5° (for 4.6 ms, 0.78 V rf pulse). In Figure 5**a** a typical, slightly off-resonance NMR signal observed at the output of the NMR polarimeter is shown, whereas the Fig. 5**b** indicates the flip angle calibration curve.

The rf flip angle calibration was taken into account during the following T_1 measurement. The longitudinal relaxation time T_1 is one of the crucial parameters for

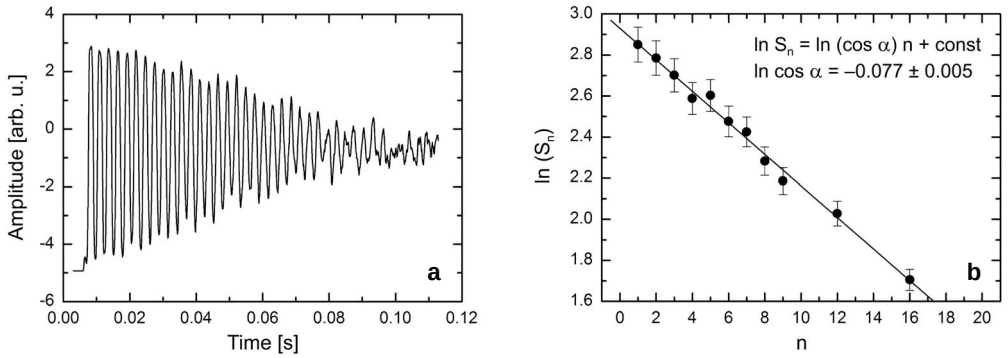

Fig. 5. Typical free induction decay (FID) signal from hyperpolarized ^{3}He obtained at magnetic field of about 25 G (the Larmor frequency is equal to 82.8 kHz, the rf pulse width was set to 4.6 ms and amplitude to 0.78 V) – **a**. Flip angle calibration gives the value of tilting angle for rf pulse to be 22.5° for 4.6 ms, and 0.78 V – **b**.

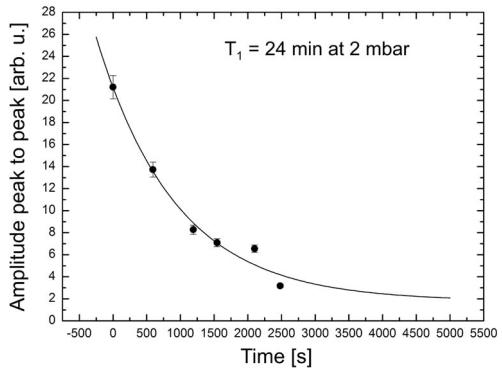

Fig. 6. T_1 measurement for pure ^{3}He at 2 mbar.

the hyperpolarized gas production, since it imposes both an upper limit for achievable polarization in the OP cell, and the maximum gas storage time. In our system the spin -lattice relaxation time T_1 in the pure ^{3}He gas at 2 mbar measured by a series of small tilting angle rf pulses was equal to 24 min (Fig. 6)

To optimise the performance of the polarizer, the dynamics of the optical pumping process in the OP cell was measured by means of optical method (Fig. 7). The first part of the curve shows the exponential growth of polarization when the pumping beam is applied. The characteristic pumping time of about 9 s is determined from the plot. When the nuclear polarization reaches its steady state value of about 30%, the laser beam is blocked and the relaxation caused mostly by the discharge is observed. The build-up time and the relaxation time both depend on the gas pressure and intensity of the discharge. It has been found that for the given pressure of 1 mbar the pumping time and the relaxation time can vary in the range of 9–30 s, and 16–95 s, respectively, decreasing with the discharge intensity.

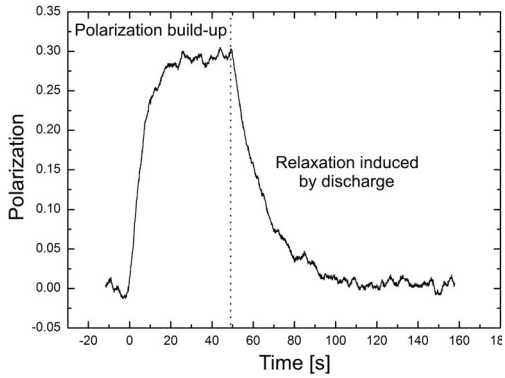

Fig. 7. Example of optical pumping dynamics for pure ^{3}He gas inside OP cell at pressure of about 1 mbar. The characteristic build-up time constant is equal to 9 s, and the relaxation induced by discharge is 16 s. The discharge of strong intensity was used. The 1083 nm laser was tuned to C_9 transition. The steady-state value of nuclear polarization determined from the measurement is about 30%.

The performance of the polarizer has to be optimised with respect to the total pumping time in the OP cell, and the relaxation time in the S cell. Since the whole polarization process has to be completed in time shorter than T_1 in the storage cell, we chose the plasma intensity which results in the optical pumping time of 15 s. Right after the completion of the optical pumping the output valve of the OP is opened and the gas is transported into the storage cell in about 1 min. The pressure inside the storage cell is increasing by 5 mbar after every repumping cycle. In the last step the OP cell is refilled with the new portion of gas. We normally perform about 20 compression cycles to reach the pressure of 100 mbar in the storage cell. Then the buffer gas (^{4}He or N_2) is added to reach the atmospheric pressure. The gas prepared in this way can be later extracted into the syringe and transported into the MRI scanner for imaging.

In order to evaluate the performance of the polarizing unit equipped with the compressor, we performed several experiments in the low-field MRI scanner. As a first phantom a 75 ml glass cell filled with a mixture of ^{3}He and ^{4}He at the atmospheric pressure was used. Transverse and sagittal images (Fig. 8) were obtained using FLASH (fast low angle shot) sequence [19] with a flip angle of about 6°, using very short repetition and echo times (TR = 16 ms, TE = 10 ms, total acquisition time = 1.1 s). For testing purposes the same technique was then applied to obtain images of the 20 ml syringe (Fig. 9**b**) which was used to extract the gas from the storage cell and to carry it to the magnet. Inside the magnet, the relaxation time T_1 in the syringe was measured to be about 5 min. Although the relaxation is relatively fast, we still have enough time to perform the imaging experiment using fast sequences. To emulate the rat lungs, the polarized ^{3}He gas was injected into a small balloon and the image of the baloon was taken (Fig. 9**c**). Finally, *in-vivo* MRI images of the anaestesized rat were obtained (Fig. 10). For imaging, the rat was tracheotomized and placed in a home-built animal bed in the centre of the rf coil, in a supine position. A volume of about 7 cm^3 of

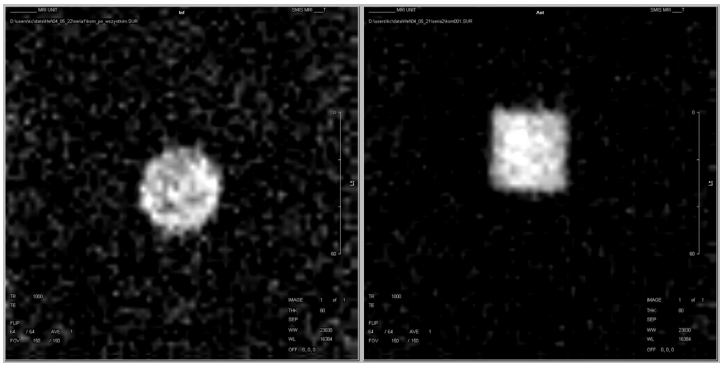

Fig. 8. Transverse and sagittal glass cell images acquired with the FLASH sequence (80 mm slice thickness, field of view = 150 mm, 64×64 voxels, flip angle 6°, no averaging, echo time = 10 ms, repetition time = 17 ms, total acquisition time = 1.1 s).

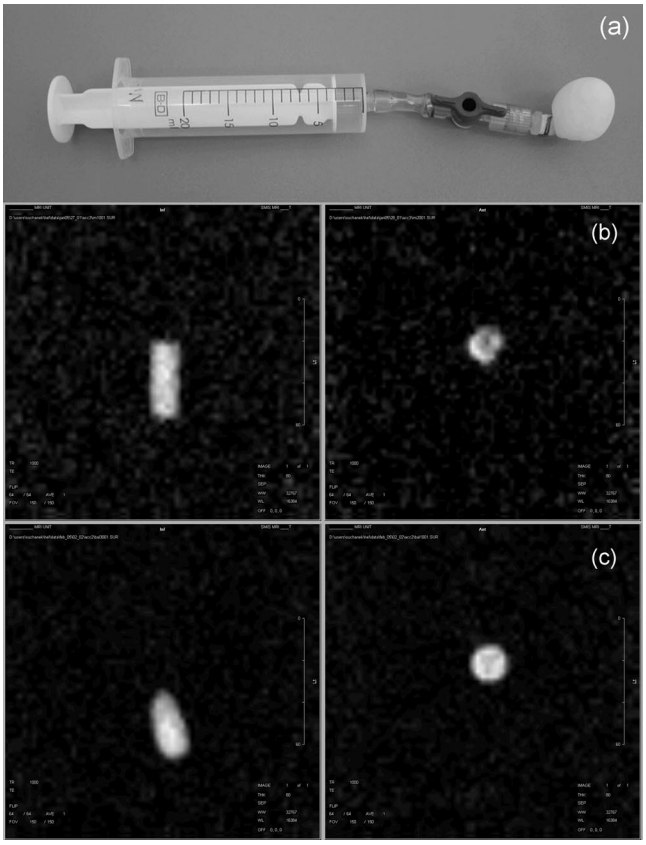

Fig. 9. Syringe with inflammable balloon (**a**). Transverse and sagittal images of the syringe (**b**) and of a small balloon (**c**) obtained with the FLASH sequence (80 mm slice thickness, field of view = 150 mm, 64×64 voxels, flip angle 6°, no averaging, echo time = 10 ms, repetition time = 17 ms, total acquisition time = 1.1 s).

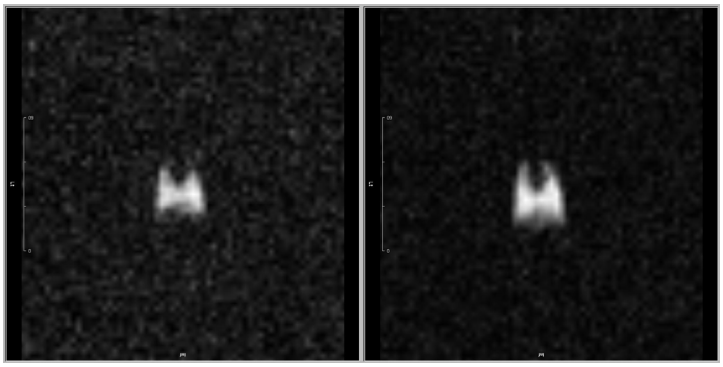

Fig. 10. Transverse ^{3}He images of rat lungs *in vivo* acquired with the FLASH sequence (80 mm slice thickness, field of view = 150 mm, 128×128 voxels, flip angle 6°, no averaging, echo time = 16 ms, repetition time = 30 ms, total acquisition time = 3.8 s).

polarized gas was introduced from the syringe into the rat lungs through the trachea catheter. The images taken after two consecutive breaths are shown on left and right of Fig. 10, respectively. In spite of low spatial resolution of these images, one can easily recognize the characteristic shape of the rat lungs.

In this work we presented a home-built portable optical polarizer with compressor which is capable of producing large amount of optically polarized ^{3}He gas using low power (50 mW) laser diode. With this device we were able to obtain the preliminary images of phantoms as well as *in vivo* images of the rat lungs. These results show the diagnostic potential of hyperpolarized ^{3}He imaging at low magnetic field (88 mT). An improvement of the image resolution and signal to noise ratio (SNR) is possible by increasing the attainable nuclear polarization of ^{3}He and the gas production rate. A straightforward way to achieve this goal is to use a more powerful laser source [20]. Another approach is to perform optical pumping at higher filed. It has been found that the process is very efficient even for high gas pressures at the standard field of a medical scanner (1.5 T) [21, 22]. The reported maximum polarization is 24% at 67 mbar. The advantage of optical pumping at high gas pressure is that the compression rate needed can be much smaller or the buffer gas can be added directly after one run of optical pumping. Hence the whole procedure can be made much shorter with less severe polarization losses. Moreover, it will be possible to polarize gas inside the medical scanner right before imaging experiments. We are currently trying to find the optimal conditions for this process for different gas pressures and magnetic field strengths using a superconducting magnet capable of giving the maximum field of 2 T and several sealed gas cells with fixed pressures.

Acknowledgement – We express our gratitude to P.J. Nacher and his group from ENS, Paris, France for lending us several components that were essential for building the polarizing unit. We thank K. Majcher and P. Marcinek for their help with animal preparation. This work was supported in part by the E.C. Fifth

Framework Program (PHIL project QLG1-2000-01559), the Polish State Committee for Scientific Research (grant no. 158/E-338/SPUB-M/5 PR UE/DZ 82/2001-03), and the Polish Science Foundation (SUBIN no. 17/98, MILAB no. 40/2002).

References

[1] MOLLER H.E., CHEN X.J., SAAM B., HAGSPIEL K.D., JOHNSON G.A., ALTES T.A., DE LANGE E.E., KAUCZOR H.-U., *MRI of the lungs using hyperpolarized noble gases*, Magnetic Resonance in Medicine **47**(6), 2002, pp. 1029–51.

[2] ISHII M., ROBERTS D.A., LOOBY P.G., EDVINSSON J., JALALI A., RIZI R., *^{3}He MR imaging of porcine paranasal sinuses*, Academic Radiology **10**(4), 2003, pp. 373–8.

[3] GUILLOT G., NACHER P.-J., TASTEVIN G., *NMR diffusion of hyperpolarised ^{3}He in aerogel: a systematic pressure study*, Magnetic Resonance Imaging **19**(3-4), 2001, pp. 391–4.

[4] MIDDLETON H., BLACK R.D., SAAM B., CATES G.D., COFER G.P., GUENTHER R., HAPPER W., HEDLUND L.W., JOHNSON G.A., JUVAN K., SWARZ J., *MR imaging with hyperpolarized ^{3}He gas*, Magnetic Resonance in Medicine **33**(2), 1995, pp. 271–5.

[5] EBERT M., GROSSMANN T., HEIL W., OTTEN E.W., SARKAU R., LEDUC M., BACHERT P., KNOPP M.V., SCHAD L.R., THELEN M., *Nuclear magnetic resonance imaging with hyperpolarised helium-3*, Lancet **347**(9011), 1996, pp. 1297–9.

[6] BACHERT P., SCHAD L.R., BOCK M., KNOPP M.V., EBERT M., GROSSMANN T., HEIL W., HOFFMAN D., SURKAU R., OTTEN E.W., *Nuclear magnetic resonance imaging of airways in humans with use of hyperpolarized ^{3}He*, Magnetic Resonance in Medicine **36**(2), 1996, pp. 192–6.

[7] CRÉMILLIEUX Y., BERTHEZENE Y., HUMBLOT H., VIALLON M., CANET E., BOURGEOIS M., ALBERT T., HEIL W., BRIGUET A., *A combined ^{1}H perfusion/^{3}He ventilation NMR study in rat lungs*, Magnetic Resonance in Medicine **41**(4), 1999, pp. 645–8.

[8] WOODS J.C., YABLONSKIY D.A., CHINO K., TANOLI T.S.K., COOPER J.D., CONRADI M.S., *Magnetization tagging decay to measure long-range (3)He diffusion in healthy and emphysematous canine lungs*, Magnetic Resonance in Medicine **51**(5), 2004, pp. 1002–8.

[9] KASTLER A., *Quelques suggestions concernant la production optique et la détection optique d'une inégalité de population des niveaux de quantification spatiale des atomes. Application a l'expérience de Stern et Gerlach et a la résonance magnétique*, J. Phys. Radium **11**(6), 1950, pp. 255–6.

[10] WONG G.P., TSENG C.H., POMEROY V.R., MAIR R.W., HINTON D.P., HOFFMAN D., STONER R.E., HERSMAN F.W., CORY D.G., WALSWORTH R.L., *A system for low field imaging of laser-polarized noble gas*, Journal of Magnetic Resonance **141**(2), 1999, pp. 217–27.

[11] DARRASSE L., GUILLIOT G., NACHER P.-J., TASTEVIN G., *Low-field ^{3}He nuclear magnetic resonance in human lungs*, Comptes Rendus de l'Academie des Sciences, Serie 2b **324**, 1997, pp. 691–700.

[12] BIDINOSTI C.P., CHOUKEIFE J., NACHER P.-J., TASTEVIN G., *In vivo NMR of hyperpolarized ^{3}He in the human lung at very low magnetic fields*, Journal of Magnetic Resonance **162**(1), 2003, pp. 122–32.

[13] WALKER T. G., HAPPER W., *Spin-exchange optical pumping of noble-gas nuclei*, Reviews of Modern Physics **69**(2), 1997, p. 629–42.

[14] COLEGROVE F.D., SCHEARER L.D., WALTERS G.K., *Polarization of ^{3}He gas by optical pumping*, Physical Review **132**(6), 1963, pp. 2561–72.

[15] BOUCHIAT M.A., CARVER T.R., VARNUM C.M., *Nuclear polarization in ^{3}He gas induced by optical pumping and dipolar exchange*, Physical Review Letters **5**(8), 1960, pp. 373–5.

[16] STOLTZ E., VILLARD B., MEYERHOFF M., NACHER P.-J., *Polarization analysis of the light emitted by an optically pumped ^{3}He gas*, Applied Physics B: Lasers and Optics **63**(6), 1996, pp. 635–40.

[17] CHOUKEIFE J., MAITRE X., NACHER P.-J., TASTEVIN G., *On-site production of hyperpolarized helium-3 for lung MRI*, Magnetic Resonance Materials in Physics, Biology, and Medicine, Suppl. 1 to Vol. 15, 2002, p. 201.

[18] SUCHANEK M., CIEŚLAR K., PAŁASZ T., SUCHANEK K., DOHNALIK T., OLEJNICZAK Z., *Magnetic resonance imaging at low magnetic field using hyperpolarized ^{3}He gas*, Acta Physica Polonica A **107**(3), 2005, pp. 491–506.

[19] HAASE A., FRAHM J., MATTHAEI D., HANICKE W., MERBOLDT K.-D., *FLASH imaging. Rapid NMR imaging using low flip-angle pulses*, Journal of Magnetic Resonance **67**(2), 1986, pp. 258–66.

[20] GENTILE T.R., HAYDEN M.E., BARLOW M.J., *Comparison of metastability-exchange optical pumping sources*, Journal of the Optical Society of America B: Optical Physics **20**(10), 2003, pp. 2068–74.

[21] ABBOUD M., SINATRA A., MAITRE X., TASTEVIN G., NACHER P.J., *High nuclear polarization of ^{3}He at low and high pressure by metastability exchange optical pumping at 1.5 tesla*, Europhysics Letter **68**(4), 2004, pp. 480–6.

[22] COURTADE E., MARION F., NACHER P.J., TASTEVIN G., KIERSNOWSKI K., DOHNALIK T., *Magnetic field effects on the 1 083 nm atomic line of helium – Optical pumping of helium and optical polarisation measurement in high magnetic field*, The European Physical Journal D **21**(1), 2002, pp. 25–56.

Received March 19, 2005